Quantum Corrections to Classical BGK Modes in Phase Space

Lucio Demeio[1]

[1]Dipartimento di Scienze Matematiche
Universitá Politecnica delle Marche
Via Brecce Bianche 1, 60131 Ancona - Italy
e-mail: demeio@mta01.univpm.it

ABSTRACT

In this paper we study the quantum corrections to the Bernstein-Greene-Kruskal equilibria of plasma physics by using perturbation methods near the classical solution. We obtain the solution for the Wigner function and for the self-consistent potential to first order in the smallness parameter, which is the square of Planck's constant (in dimensionless form), and investigate the structure of the quantum phase space.

1 Introduction

The steady-state solutions of the Vlasov-Poisson system [1] with periodic boundary conditions, also called BGK modes or BGK equilibria [2], have been studied extensively over the years and their importance in the theory of plasma waves is well established [3]. In 1996, Lange, Toomire and Zweifel [4] introduced a quantum generalization of BGK equilibria, by proving the existence and uniqueness of the steady-state solutions of the Wigner-Poisson system with periodic boundary conditions, and called these solutions Quantum BGK (QBGK) modes. In solid-state physics, the Wigner-Poisson system is usually equipped with inflow boundary conditions and periodic boundary conditions are of little importance in the applications to real systems. The motivation for studying QBGK modes lies mainly in their theoretical interest and in the fact that they possess a well-known classical limit.

The Wigner-Poisson system is the quantum analogue of the Vlasov-Poisson system [5, 6]; the Wigner equation is the governing equation for the Wigner function, and has the important property that its solutions tend to the solutions of the Vlasov equation in the

classical limit [7]. A full characterization of QBGK modes requires the numerical solution of the steady-state Wigner-Poisson system, which is a difficult task and we leave it for a second paper. In this paper, we take a simpler approach, by using a perturbative expansion of the Wigner function and of the self-consistent potential about the classical solution, by introducing a smallness parameter proportional to the square of Planck's constant. This methodology is often used in the literature (see, for example, [8, 9]) in order to investigate the behaviour of quantum systems near the classical limit; it mainly has two shortcomings: it cannot be used very far into the quantum regime (since it is a perturbative approach), and it also bypasses the delicate question of the classical limit of Quantum Mechanics. Therefore, it can only provide a glimpse of the quantum behaviour of the physical system. The advantage of using the perturbative approach lies in its simplicity and in the possibility of obtaining analytical expressions. In particular, the results of the perturbative approach can be interpreted in the language of phase space; the quantum phase-space orbits are often intrpreted as classical orbits with a quantum correction. As we shall see with our kinetic model, however, non-classical features appear in the phase-space orbits also when the smallness parameter is very close to zero.

2 The Vlasov-Poisson and the Wigner-Poisson systems

In this work, we study the quantum corrections to the Bernstein-Greene-Kruskal equilibria (BGK modes) that arise in the nonlinear theory of collisionless plasma waves. These phenomena are usually described by the Vlasov-Poisson system [1]

$$\frac{\partial f}{\partial t} + p\frac{\partial f}{\partial x} - E\frac{\partial f}{\partial p} = 0 \tag{1}$$

$$\frac{\partial E}{\partial x} = 1 - \int f dp, \tag{2}$$

which governs the time evolution of the electron distribution function $f(x,p,t)$ and of the self-consistent electric field $E(x,t)$ generated by the space-charge separation due to the motion of the electrons with respect to the fixed background of the ions. Equations (1)-(2) are written in dimensionless form: the space variable x, the momentum variable p and the time variable t are measured in units of the Debye length $\lambda_D = \sqrt{T/(4\pi ne^2)}$, the thermal momentum mv_{th}, with $v_{th} = \sqrt{T/m}$ the thermal speed, and of the inverse plasma frequency $\omega_p^{-1} = \lambda_D/v_{th}$, respectively. Also, f is measured in units of $n/(mv_{th})$ and E in units of $4\pi ne\lambda_D$ (m is the electron mass, e the electron charge, T the plasma temperature and n the plasma density). When the Vlasov-Poisson system (1)-(2) is used to describe plasma waves, periodic conditions in space are imposed, $f(x,p,t) = f(x+L,p,t)$ and $E(x,t) = E(x+L,t)$, where L is the periodicity length. The boundary conditions in momentum follow from the assumption that all the moments of the distribution function, $M_n(x,t) = \int p^n f(x,p,t)\, dp$, exist. The solutions of the steady-state Vlasov-Poisson system

$$p\frac{\partial f}{\partial x} - E\frac{\partial f}{\partial p} = 0 \tag{3}$$

$$\frac{\partial E}{\partial x} = 1 - \int f dp, \tag{4}$$

are called BGK equilibria. They can be lifted to solutions of the time-dependent Vlasov-Poisson system (1)-(2) by Galilean transformations with arbitrary phase speed.

The Wigner-Poisson system is the quantum analogue of the Vlasov-Poisson system (1)-(2). The solutions of the steady-state Wigner-Poisson system with periodic boundary conditions, which we investigate here, are called Quantum BGK modes and have been introduced by Lange, Toomire and Zweifel [4].

In order to set up the Wigner-Poisson system and to introduce consistently the dimensionless variables, we begin with the Schrödinger equation for a single electron of mass m

$$i\hbar\frac{\partial \psi}{\partial t} = -\frac{\hbar^2}{2m}\frac{\partial^2 \psi}{\partial x^2} + V\psi,$$

where $V(x)$ is the electrostatic potential energy, and then define the density matrix in the space representation. For a mixture of states ψ_m, with weights λ_m, $m = 0, 1, \ldots$, the density matrix ρ is given by

$$\rho(x, y) = \sum_m \lambda_m \psi_m(x)\psi_m^*(y). \tag{5}$$

By using the dimensionless variables introduced above, we write the Schrödinger equation in dimensionless form

$$i\tilde{\varepsilon}\frac{\partial \psi}{\partial t} = -\frac{\tilde{\varepsilon}^2}{2}\frac{\partial^2 \psi}{\partial x^2} + V\psi, \tag{6}$$

where the potential energy is now measured in units of mv_{th}^2 and $\tilde{\varepsilon} = \hbar/(mv_{th}\lambda_D)$ is the dimensionless Planck constant. This definition for the dimensionless Planck constant is merely a consequence of our choice of the dimensionless variables and is not to be considered a universal parameter that describes the importance of quantum effects in a quantum plasma in general; in the modelling of quantum plasmas [10], other parameters are frequently used, often involving the Fermi energy. Typical values of the parameter $\tilde{\varepsilon}$ are $\tilde{\varepsilon} \sim 10^{-6}$ for fusion plasmas, $\tilde{\varepsilon} \sim 10^{-12}$ for space plasmas and $\tilde{\varepsilon} \sim 1$ in semiconductors. We introduce the Wigner function of the mixture by

$$f_W(x, p) = \frac{1}{2\pi\hbar}\int d\eta \rho\left(x + \frac{\eta}{2}, x - \frac{\eta}{2}\right) e^{-ip\eta/\hbar}$$

which, in our dimensionless units, becomes

$$f_W(x, p) = \frac{1}{2\pi}\int d\tau \rho\left(x + \frac{\tilde{\varepsilon}\tau}{2}, x - \frac{\tilde{\varepsilon}\tau}{2}\right) e^{-ip\tau}, \tag{7}$$

where p is the dimensionless Wigner momentum variable measured in units of mv_{th}. In dimensionless units, the Fourier transform of the Wigner function is

$$\widehat{f}_W(x, \tau) = \int dp f_W(x, p) e^{ip\tau} = \rho\left(x + \frac{\tilde{\varepsilon}\tau}{2}, x - \frac{\tilde{\varepsilon}\tau}{2}\right). \tag{8}$$

Note that

$$\int f_W(x,p)dp = n(x) \tag{9}$$

gives the number density:

$$\begin{aligned}\int f_W(x,p)dp &= \frac{1}{2\pi}\int d\tau \rho\left(x+\frac{\tilde{\varepsilon}\tau}{2}, x-\frac{\tilde{\varepsilon}\tau}{2}\right) 2\pi\delta(\tau) = \\ &= \rho(x,x) = \sum_m \lambda_m |\psi_m(x)|^2 = n(x).\end{aligned}$$

The evolution equation for the Wigner function in dimensionless units is

$$\frac{\partial f_W}{\partial t} + p\frac{\partial f_W}{\partial x} + \frac{i}{\tilde{\varepsilon}}\Theta(\delta V) f_W = 0 \tag{10}$$

where the pseudodifferential operator Θ, in dimensionless units, is given by

$$(\Theta(\delta V) f_W)(x,p) = \frac{1}{2\pi}\int d\tau \delta V(x,\tau)\widehat{f}_W(x,\tau)e^{-ip\tau}, \tag{11}$$

with symbol $\delta V(x,\tau) = V(x+\tilde{\varepsilon}\tau/2) - V(x-\tilde{\varepsilon}\tau/2)$. If we use the electrostatic potential ϕ instead of the potential energy V, equation (10) becomes

$$\frac{\partial f_W}{\partial t} + p\frac{\partial f_W}{\partial x} - \frac{i}{\tilde{\varepsilon}}\Theta(\delta\phi) f_W = 0, \tag{12}$$

since in our dimensionless units we simply have $\phi(x) = -V(x)$.

We now turn to Poisson's equation,

$$\frac{\partial E}{\partial x} = 4\pi e(n_0 - \rho(x,x)),$$

where $E(x) = -d\phi/dx$ is the electric field. In dimensionless units this becomes

$$\frac{\partial E}{\partial x} = 1 - \rho(x,x),$$

where the electric field is measured in units of $4\pi n_0 e\lambda_D$ and the density matrix ρ in units of the ion density n_0. With these dimensional normalizations, the Wigner function f_W is measured in units of $n_0/(mv_{th})$. The Wigner-Poisson system in the dimensionless units is then

$$\frac{\partial f_W}{\partial t} + p\frac{\partial f_W}{\partial x} - \frac{i}{\tilde{\varepsilon}}\Theta(\delta\phi) f_W = 0 \tag{13}$$

$$\frac{\partial E}{\partial x} = 1 - \int f_W dp, \tag{14}$$

which is the quantum analogue of the Vlasov-Poisson system (1)-(2). We impose periodic boundary conditions, $f_W(x,p,t) = f_W(x+L,p,t)$ and $E(x,t) = E(x+L,t)$, where L

is the periodicity length. Like in the case of the Vlasov-Poisson system, the boundary conditions in momentum follow from the assumption that all the moments of the Wigner function, $M_n(x,t) = \int p^n f_W(x,p,t)\, dp$, exist. The QBGK equilibria introduced in [4] are the steady-state solutions of the Wigner-Poisson system (13)-(14) with periodic boundary conditions.

Before illustrating the perturbative solution, we would like to mention some important properties of the Wigner-Poisson system.

Both the Vlasov-Poisson and the Wigner-Poisson systems are invariant under Galilean transformations with arbitrary phase velocity. Thus, steady-state solutions (equilibria) of either (VP) or (WP) can be lifted to travelling waves (modes), that is solutions of the corresponding time-dependent systems. In this paper, we are only concerned with BGK and QBGK equilibria.

In the presence of a periodic potential, Bloch's theorem holds and the Hamiltonian corresponding to QBGK equilibria has a complete set of Bloch eigenfunctions $\Psi_{mk}(x)$ and energy bands $\epsilon_m(k)$ (k is the quasi-momentum). Also, in a steady state, the density operator commutes with the Hamiltonian and is therefore diagonal in the Bloch functions' basis. It is easy to see that, as a consequence, the Wigner function automatically becomes an $L-$periodic function of x.

When the problem is studied at the Schrödinger level, the periodicity of the wave function $\psi(x)$ in space is often imposed. This condition, which is not necessary to ensure the periodicity of the Wigner function, bears the consequence that both the quasi-momentum k and the phase-space momentum variable p are quantized, i.e. they can only take discrete sets of values. The Wigner function is then defined by a Fourier series in momentum rather than the usual Fourier transform.

3 The perturbative solution

The steady-state Wigner-Poisson system is the quantum analogue of the steady-state Vlasov-Poisson system and is given by

$$p\frac{\partial f_W}{\partial x} - \frac{i}{\tilde{\epsilon}}\Theta(\delta\phi) f_W = 0 \tag{15}$$

$$\frac{\partial E}{\partial x} = 1 - \int f_W\, dp, \tag{16}$$

where all the symbols have already been defined. We shall study the solutions of the system (15)-(16) with periodic boundary conditions for small $\tilde{\varepsilon}$ by using a perturbation expansion about the classical solution. To this aim, we begin by introducing the Moyal expansion for the pseudodifferential operator Θ:

$$-\frac{i}{\tilde{\epsilon}}\Theta(\delta\phi) f_W(x,p) = -E(x)\frac{\partial f_W}{\partial p} + \frac{\tilde{\epsilon}^2}{24}\frac{\partial^2 E}{\partial x^2}\frac{\partial^3 f_W}{\partial p^3} + \mathcal{O}(\tilde{\epsilon}^4). \tag{17}$$

By setting $\varepsilon = \tilde{\varepsilon}^2/24$, the steady-state Wigner-Poisson system (15)-(16) becomes:

$$p\frac{\partial f_W}{\partial x} - E(x)\frac{\partial f_W}{\partial p} + \varepsilon\frac{\partial^2 E}{\partial x^2}\frac{\partial^3 f_W}{\partial p^3} + \mathcal{O}(\varepsilon^2) = 0 \tag{18}$$

$$\frac{\partial E}{\partial x} = 1 - \int f_W dp. \tag{19}$$

Equation (18) is the asymptotic form of the Wigner equation for $\epsilon \to 0$. It clearly has the form of the classical equation with a first-order quantum correction. The quantum correction is proportional to the third derivative of the Wigner function with respect to p and, most importantly, is proportional to the second derivative of the electric field, that is the second derivative of the force acting on the single particle. This is related to the well known fact that, in the governing equation for the Wigner function in presence of linear or quadratic potentials, quantum effects are absent.

We now introduce a perturbative expansion of f_W and ϕ in powers of ε:

$$f_W(x,p) = f_0(x,p) + \varepsilon f_1(x,p) + \mathcal{O}(\varepsilon^2) \tag{20}$$

$$\phi(x) = \phi_0(x) + \varepsilon\phi_1(x) + \mathcal{O}(\varepsilon^2). \tag{21}$$

The expansion of the potential (21) induces an analogous expansion of $E(x) = -\phi'(x)$: $E(x) = E_0(x) + \varepsilon E_1(x) + \mathcal{O}(\varepsilon^2)$, where $E_n(x) = -\phi_n'(x)$, $n = 0, 1, \ldots$.

By substituting into (18)-(19), to order ε^0 we have:

$$p\frac{\partial f_0}{\partial x} - E_0\frac{\partial f_0}{\partial p} = 0 \tag{22}$$

$$\frac{\partial E_0}{\partial x} = 1 - \int f_0 dp, \tag{23}$$

which is the classical steady-state Vlasov-Poisson system and, to order ε, we have:

$$p\frac{\partial f_1}{\partial x} - E_0\frac{\partial f_1}{\partial p} - E_1\frac{\partial f_0}{\partial p} + \frac{\partial^2 E_0}{\partial x^2}\frac{\partial^3 f_0}{\partial p^3} = 0 \tag{24}$$

$$\frac{\partial E_1}{\partial x} = -\int f_1 dp. \tag{25}$$

The zero-order solution $(f_0(x,p), E_0(x))$ is therefore a classical BGK equilibrium. The first-order system (24)-(25) needs to be equipped with boundary conditions. We choose to impose the boundary conditions so that the total quantum solution, to first order in ε, coincides with classical solution at $x = 0$ and $x = L$, and therefore has the same periodicity length of the classical solution. Of course, one can think of a different set of boundary conditions and obtain a different QBGK equilibrium, which will have the same classical limit. For example, we could impose $\phi_1(0) = \phi_1'(0) = 0$, which would lead to a QBGK equilibrium with a slightly different periodicity length from the one of the zero-order classical solution [11]. Therefore, in the neighbourhood of a classical BGK equilibrium, there exist many QBGK equilibria all having the same classical limit.

3.1 Zero-order solution: Classical BGK modes

The solution of the zero-order system (22)-(23) is a classical BGK equilibrium, which we construct by following the methodology outlined in [12] and in [13], and which we recall here for clarity. The solution is obtained by first assigning the distribution over the whole phase space as a functional of the potential, and then by solving Poisson's equation for the potential.

A large class of solutions of the steady-state Vlasov-Poisson system (22)-(23) is obtained by considering functions $f_0(x,p) = F_0(\mathcal{E})$, where $\mathcal{E} \equiv p^2/2 - \phi_0(x)$ is the single-particle energy, with $\phi_0(x) = -\int^x E_0(x')\,dx'$ the electrostatic potential. Any such function $F_0(\mathcal{E})$ satisfies the steady-state Vlasov equation (22) identically. The electrostatic potential $\phi_0(x)$ partitions the electron population into three groups of particles: trapped particles, untrapped particles with positive momentum and untrapped particles with negative momentum. The curves that divide the trapped and untrapped populations of the phase space are separatrices of a given energy ϵ_s. Then, one can think of a problem with four components: the three groups of particles and the electrostatic potential. In general, three of these components can be fixed with some arbitrariness and the fourth one is then found by solving the equations. In our approach, we assign the distribution function over the entire phase space; Poisson's equation then becomes a differential equation for the electrostatic potential $\phi_0(x)$. The distribution function is first assigned at one boundary, $x = 0$, by $f_0(0,p) = m(p)(1+\alpha)$, for a given function $m(p)$ and α arbitrary. In general, ϵ_s and α are positive numbers, with $\alpha << 1$. As they vary, a family of BGK equilibria is obtained, which we call the BGK equilibria generated by the function $m(p)$. The electrostatic potential is subject to the boundary conditions $\phi_0(0) = -\epsilon_s$ and $\phi_0'(0) = 0$. These boundary conditions and the numerical generation of BGK modes are discussed in more detail in [13]. If $\phi_0(x)$ is the unknown electrostatic potential, the equations of the separatrices are given by

$$p(x) = \pm\sqrt{2(\phi_0(x) + \epsilon_s)} = \pm p_0(x).$$

Then for $-p_0(x) < p < p_0(x)$ (trapped particles) the distribution is left arbitrary, $f_0(x,p) = F_t(\mathcal{E})$, and for $p < -p_0(x)$ or $p > p_0(x)$ (untrapped particles) we take $f_0(x,p) = f_0(0,\bar{p})$, where $\bar{p}$ is the momentum obtained by considering the constant energy curve passing through the point (x,p) of the phase space and tracing it back to $x = 0$. The value of $\bar{p}$ is determined by $p^2/2 - \phi_0(x) = \bar{p}^2/2 + \epsilon_s$. Summarizing, $f_0(x,p) = F_0(\mathcal{E})$ where

$$F_0(\mathcal{E}) = \begin{cases} F_-(\mathcal{E}) = f_0\left(0, -\sqrt{2(\mathcal{E}-\epsilon_s)}\right), & \mathcal{E} > \epsilon_s \text{ and } p < -p_0(x) \\ F_t(\mathcal{E}), & -\phi_{MAX} < \mathcal{E} < \epsilon_s \\ F_+(\mathcal{E}) = f_0\left(x, \sqrt{2(\mathcal{E}-\epsilon_s)}\right), & \mathcal{E} > \epsilon_s \text{ and } p > p_0(x) \end{cases} \tag{26}$$

where ϕ_{MAX} is the maximum value of the potential ϕ_0. The distribution function thus constructed is a functional of the electrostatic potential $\phi_0(x)$. Therefore, Poisson's equation can be written as:

$$-\frac{d^2\phi_0}{dx^2} = 1 - \mathcal{R}(\phi_0) \tag{27}$$

with $\mathcal{R}(\phi_0) = \int f_0(x,p)dp = \int ||J||_{\phi_0} F_0(\mathcal{E})d\mathcal{E}$, where $||J||_\psi$ is the Jacobian of the transformation from the momentum variable to the energy variable for fixed x and a general electrostatic potantial ψ. For an arbitrary function $w(x,p) = W(\mathcal{E})$, we have

$$\begin{aligned}\int_{-\infty}^{+\infty} w(x,p)dp = \int ||J||_\psi W(\mathcal{E})d\mathcal{E} &= \int_{\epsilon_s}^{\infty} \frac{(W_-(\mathcal{E}) + W_+(\mathcal{E}))d\mathcal{E}}{\sqrt{2(\mathcal{E}+\psi(x))}} + \\ &+ 2\int_{-\psi(x)}^{\epsilon_s} \frac{W_t(\mathcal{E})d\mathcal{E}}{\sqrt{2(\mathcal{E}+\psi(x))}} \end{aligned} \tag{28}$$

where W_+, W_- and W_t correspond to the untrapped (with $p > 0$ and $p < 0$) and trapped particles, respectively. Then,

$$\mathcal{R}(\phi_0) = \int_{\epsilon_s}^{\infty} \frac{(F_-(\mathcal{E}) + F_+(\mathcal{E}))d\mathcal{E}}{\sqrt{2(\mathcal{E}-\phi_0)}} + 2\int_{-\phi_0(x)}^{\epsilon_s} \frac{F_t(\mathcal{E})d\mathcal{E}}{\sqrt{2(\mathcal{E}-\phi_0)}}. \tag{29}$$

With this expression, eq. (27) becomes a second order differential equation for the potential $\phi_0(x)$, equipped with the boundary conditions $\phi_0(0) = -\epsilon_s$ and $\phi_0'(0) = 0$. In our numerical approach, the integrals appearing in (29) are calculated by standard Laguerre and Chebychev collocation rules and the differential equation for the potential is solved by using a standard marching technique from the boundary at $x = 0$. The periodicity length L is then extracted from the solution of the differential equation by using the condition $\phi_0(L) = \phi_0(0)$. In our former calculations of classical BGK modes [13], the computed period was consistent with the periodicity length determined by using the potential theory for BGK modes (see [2] and [3]). The amplitude of the potential is governed by the parameter α. For $\alpha = 0$ we have $f(0,p) = m(p)$ and the only solution is the one with zero field and a uniform distribution. As α becomes positive, a BGK mode with nonzero field amplitude is generated.

In this work we use the BGK equilibrium generated by the two-stream distribution,

$$f_0(0,p) = (1+\alpha)m(p) \tag{30}$$

where

$$m(p) \equiv \frac{1}{2\sqrt{2\pi}}\left[e^{-(p-p_s)^2/2} + e^{-(p+p_s)^2/2}\right] \tag{31}$$

with $p_s = 2$ and $\alpha = 0.1$. The trapped particle distribution must be chosen so that the existence conditions for the classical BGK equilibrium that gives the zero-order solution are satisfied [3]. We take

$$F_t(\mathcal{E}) = f_0(0,0)e^{\beta_1(\mathcal{E}-\mathcal{E}_s)+\beta_2(\mathcal{E}-\mathcal{E}_s)^2+\beta_3(\mathcal{E}-\mathcal{E}_s)^3+\beta_4(\mathcal{E}-\mathcal{E}_s)^4}, \tag{32}$$

with β_i, $i = 1,\ldots 4$, determined by continuity of the function and of the first three derivatives at the separatrices. The reason for this choice is because the first-order solution for the Wigner function, $f_1(x,p)$, which will be derived in the next subsection, contains the derivatives of F_0, supposed continuous, up to third order. This BGK distribution is shown in Figures 1A (level curves) and 1B (3D plot).

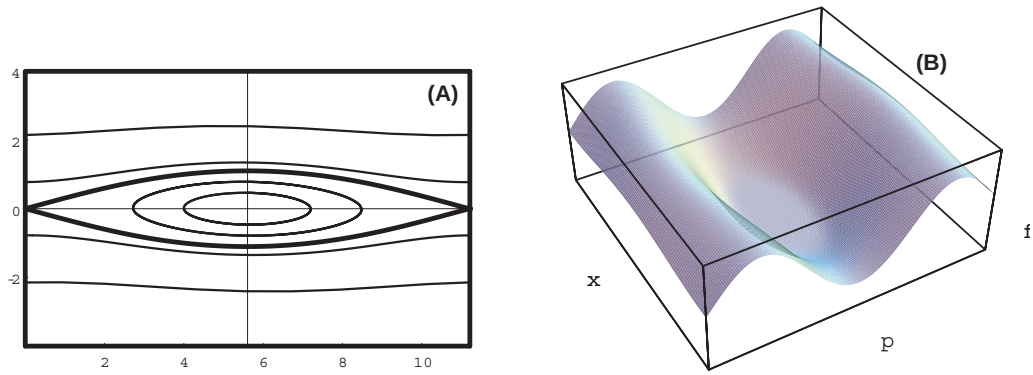

Figure 1: Phase-space orbits and distribution function of the BGK mode corresponding to the boundary condition (30)-(31) and trapped particle distribution given by (32).

3.2 First-order solution: Quantum BGK modes

The first-order solution is obtained by solving the system (24)-(25) with the boundary conditions $f_1(0,p) = 0$, $\phi_1(0) = \phi_1(L) = 0$. With this choice for the boundary conditions, the Wigner function and the potential at the $x = 0$ boundary, as well as the periodicity length L are those of the classical solution.

In order to proceed, it is convenient to adopt the transformation from the phase-space variables x and p to the variables x and $\mathcal{E}$. While the lowest order Wigner distribution is a function of $\mathcal{E}$ alone (that is $f_0(x,p) = F_0(\mathcal{E})$), the first order correction gives the variation of the Wigner function along the curves of constant $\mathcal{E}$, and so $f_1(x,p) = F_1(x,\mathcal{E})$. The partial derivatives of f_0 and f_1 in the new variables x and $\mathcal{E}$ then become:

$$\begin{aligned}
\frac{\partial f_0}{\partial p} &= p(x) F_0'(\mathcal{E}) \\
\frac{\partial^3 f_0}{\partial p^3} &= p(x) \left[p(x)^2 F_0'''(\mathcal{E}) + 3F_0''(\mathcal{E}) \right] \\
\frac{\partial f_1}{\partial x} &= \frac{\partial F_1}{\partial x} - \phi_0(x) \frac{\partial F_1}{\partial \mathcal{E}} \\
\frac{\partial f_1}{\partial p} &= p(x) \frac{\partial F_1}{\partial \mathcal{E}},
\end{aligned}$$

where $p(x) = \pm\sqrt{2[\mathcal{E} + \phi_0(x)]}$. The differential equation (24) for f_1 then becomes

$$p(x) \left[\frac{\partial F_1}{\partial x} - E_1 F_0'(\mathcal{E}) + \frac{\partial^2 E_0}{\partial x^2} \left(p(x)^2 F_0'''(\mathcal{E}) + 3F_0''(\mathcal{E}) \right) \right] = 0, \tag{33}$$

whose solution is

$$F_1(x,\mathcal{E}) = C(\mathcal{E}) \quad - \quad F_0'(\mathcal{E})\phi_1(x) + 3\phi_0''(x) F_0''(\mathcal{E}) +$$

$$- \quad \left[\phi_0'(x)^2 - 2\phi_0''(x)(\mathcal{E}+\phi_0(x))\right] F_0'''(\mathcal{E}).$$

The integration constant $C(\mathcal{E})$ can be determined from the boundary conditions. Since $f_1(0,p) = 0$, we have $F_1(0,\mathcal{E}) = 0$, and by using that $\phi_0''(0) = -\alpha$ and $\phi_1(0) = 0$, we obtain

$$C(\mathcal{E}) = -\alpha\left[3F_0''(\mathcal{E}) + 2(\mathcal{E}-\epsilon_s)F_0'''(\mathcal{E})\right]$$

and thus

$$F_1(x,\mathcal{E}) = -F_0'(\mathcal{E})\phi_1(x) + \left[3(\phi_0''(x)-\alpha)\right]F_0''(\mathcal{E}) + \\ + 2\left[\mathcal{E}(\phi_0''(x)-\alpha) + \phi_0''(x)\phi_0(x) + \alpha\epsilon_s - \frac{\phi_0'(x)^2}{2}\right]F_0'''(\mathcal{E}). \tag{34}$$

The function ϕ_1 is still unknown and must be obtained from equation (25), which involves an integration of f_1 over the momentum space. By using (28) to perform the integration in the variable $\mathcal{E}$, equation (25) becomes:

$$\frac{d^2\phi_1}{\partial x^2}(x) + \kappa^2(x)\phi_1(x) = g(x), \tag{35}$$

where $\kappa(x)$ and $g(x)$ are periodic functions of period L and are given by

$$\kappa^2(x) = \int ||J||_{\phi_0} F_0'(\mathcal{E})d\mathcal{E}$$

$$g(x) = \left[\phi_0''(x)-\alpha\right]\left[3\delta(x)+2\beta(x)\right] + 2\left[\phi_0''(x)\phi_0(x) + \alpha\epsilon_s - \frac{\phi_0'(x)^2}{2}\right]\gamma(x),$$

where

$$\delta(x) = \int ||J||_{\phi_0} F_0''(\mathcal{E})d\mathcal{E}$$

$$\beta(x) = \int ||J||_{\phi_0} \mathcal{E}F_0'''(\mathcal{E})d\mathcal{E}$$

$$\gamma(x) = \int ||J||_{\phi_0} F_0'''(\mathcal{E})d\mathcal{E}$$

are $L-$periodic functions of x. With our choice of the boundary conditions and of the zero order BGK equilibrium, we have $\kappa^2(x) > 0$ and therefore $\kappa(x)$ is real (and chosen positive). Equation (35) for ϕ_1 is solved together with the boundary conditions $\phi_1(0) = \phi_1(L) = 0$, by using standard numerical methods. Substituting for ϕ_1 in (34) gives the first-order correction f_1 to the Wigner function.

In Figures 2A and 2B we show the quantum (solid line) and the classical (dashed line) BGK potentials for our reference BGK equilibrium for $\varepsilon = 0.1$ (Figure 2A) and $\varepsilon = 0.4$ (Figure 2B) and in Figures 3A and 3B we show the classical (Figure 3A) and the quantum (Figure 3B) distributions in the trapped particle region and near the classical separatrices, where the most important quantum corrections appear to occur. The electrostatic potential is clearly flattened by the quantum effects.

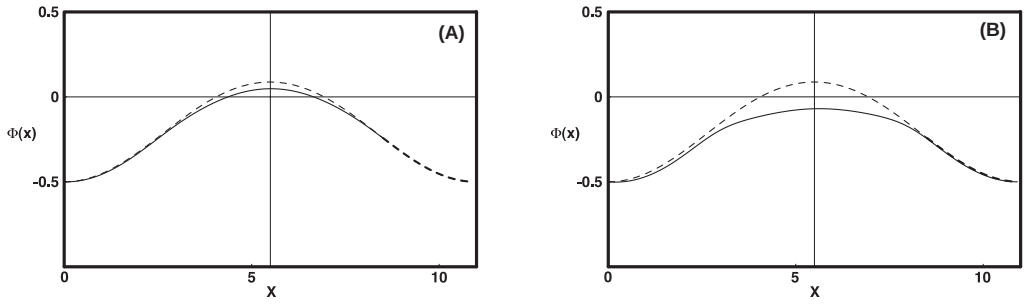

Figure 2: Classical (dashed line) and Quantum (solid line) BGK potentials for (A) $\epsilon = 0.1$ and (B) $\epsilon = 0.4$.

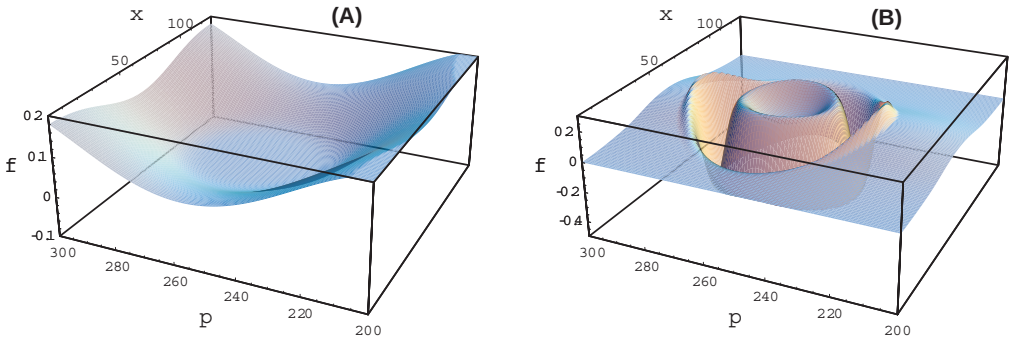

Figure 3: Classical (3A) and Quantum (3B) distributions for $\epsilon = 0.1$.

4 Classical and quantum phase-space orbits

While in classical mechanics phase-space orbits can be easily defined and a phase space can be introduced in a unique way, in quantum mechanics a different situation is encountered. The uncertainty principle makes it impossible to define the phase-space trajectories in the same way as they are defined classically, since position and momentum cannot be specified simultaneously and a quantum phase space with the same properties of the classical phase space cannot be introduced. The problem can be overcome in many different ways, and the Wigner function provides one possibility of generating a quantum phase space; other methodologies exist, such as the Husimi functions and other kind of distributions, the coherent-state reduction, the hydrodynamical approach based on the Madelung formulation of Quantum Mechanics, etc. A comparison of the advantages and disadvantages of all these different methods is out of the scope of this paper, which only uses the Wigner-function approach. Within this framework, the families of phase-space trajectories can be defined as the isolines of the Wigner function, i.e. the phase-space curves along which the Wigner function preserves its value. Here, there appears a crucial

difference with respect to the classical case: while the Vlasov equation (1) is a first-order differential equation with the associated characteristic system,

$$\dot{x} = p \tag{36}$$

$$\dot{p} = -E(x), \tag{37}$$

no such system exists for the quantum case, because the Wigner equation has a pseudodifferential structure in p. However, by introducing an effective field E_{eff} defined by

$$\frac{i}{\tilde{\varepsilon}}\Theta(\delta\phi) f_W = E_{eff}(x)\frac{\partial f_W}{\partial p},$$

a characteristic system can be introduced,

$$\dot{x} = p$$

$$\dot{p} = -E_{eff}(x),$$

where the effective field is explicitely given by

$$E_{eff}(x) = \frac{i}{\tilde{\varepsilon}}\frac{\Theta(\delta\phi) f_W}{\partial f_W/\partial p}.$$

By using the perturbation expansion (17), the effective field becomes

$$E_{eff}(x) = E(x) - \varepsilon E''(x)\frac{\partial^3 f_W/\partial p^3}{\partial f_W/\partial p} + \mathcal{O}(\varepsilon^2). \tag{38}$$

This expression for the effective field depends upon the Wigner function itself, and this shows an important difference with the classical case. While the classical phase-space structure depends only upon the shape of the potential (at least for a steady-state) and the phase-space distribution is introduced upon it, the structure of the quantum phase space depends crucially also upon the distribution. We shall see this point in more detail in the case of our model. Also, we see that the definition (38) of the effective field introduces a singularity along the lines on which $\partial f_W/\partial p = 0$. For this reason, instead of calculating the quantum phase-space orbits by using the effective field, we use our first-order analytical expression for $f_W(x,p)$, given by equation (20) together with (34), to calculate the phase-space gradient and obtain the lines of constant f_W by following, point by point, the direction orthogonal to the gradient. If the curves of constant $f_W(x,p)$ are parametrized by

$$x = x(\tau)$$

$$p = p(\tau),$$

the unit vector $\widehat{T}$ tangent to the curves is then given by

$$\widehat{T}_x = \pm\frac{\partial f_W}{\partial p}\left[\left(\frac{\partial f_W}{\partial p}\right)^2 + \left(\frac{\partial f_W}{\partial x}\right)^2\right]^{-1/2}$$

$$\widehat{T}_p = \mp\frac{\partial f_W}{\partial x}\left[\left(\frac{\partial f_W}{\partial p}\right)^2 + \left(\frac{\partial f_W}{\partial x}\right)^2\right]^{-1/2}.$$

Table 1: Critical points for $\varepsilon = 0.1$

Crit. pt.	1	2	3	4	5	6	7	8	9	10	11	12
x	0.6	0.6	2.9	2.9	5.3	5.3	5.5	5.5	8.1	8.1	11.0	11.0
p	1.8	-1.8	2.0	-2.0	2.1	-2.1	0.5	-0.5	2.0	-2.0	1.8	-1.8

and, if the parameter τ is chosen correctly, the curves are the solutions of the characteristic system

$$\frac{dx}{d\tau} = \widehat{T}_x \tag{39}$$

$$\frac{dp}{d\tau} = \widehat{T}_p \tag{40}$$

and the sign is chosen in order to obtain the correct orientation of the curve. With our perturbative approach we have:

$$\frac{\partial f_W}{\partial p} = p\left[F_0'(\mathcal{E}) + \epsilon\frac{\partial F_1}{\partial \mathcal{E}}(x,\mathcal{E})\right] + \mathcal{O}(\varepsilon^2) \tag{41}$$

$$\frac{\partial f_W}{\partial x} = E_0(x)F_0'(\mathcal{E}) + \epsilon\left[\frac{\partial F_1}{\partial x} + p\frac{\partial F_1}{\partial \mathcal{E}}(x,\mathcal{E})\right] + \mathcal{O}(\varepsilon^2) \tag{42}$$

Note that, while all the critical points of the classical characteristic system (36)-(37) lie on the $p = 0$ axis, the quantum chracteristic system (39)-(40) has also other critical points, which we have calculated numerically by using the Newton-Raphson method on our analytical solution. The critical points are shown in Table I for $\varepsilon = 0.1$. The linear analysis of the critical points, carried out by the numerical evaluation of the eigenvalues of each critical point, shows that the critical points number 3,4,9 and 10 are saddle points, the critical points number 1, 5 and 11 are stable nodes, while the critical points number 2, 6 and 12 are unstable nodes; critical points number 7 and 8 are centers. The critical points of Table I are shown in Figure 4, together with a family of phase-space orbits which we will illustrate later. On the graph, also, the two thick solid lines represent the lines along which we have $\partial f_0/\partial p = 0$. These are the lines along which the effective electric field (38) becomes singular, and are also the lines along which the relationship $F_0'(\mathcal{E}) = 0$ holds. We shall call them critical lines. Because of the way in which we have constructed our zero-order classical BGK equilibrium, these critical lines correspond to the classical phase-space trajectories along which the maxima of the two-stream distribution given by (31) are carried into the phase space for $x > 0$. It is evident that there are two subsets of critical points which lie close to the critical lines: points number 1,3,5,9 and 11 lie close to the critical line at $p > 0$, while points number 2,4,6,10 and 12 lie close to the critical line at $p < 0$. The location of these critical points near the critical lines can be understood with the following simple heuristic argument.

Suppose that we calculate the classical phase-space orbits in the same way as we calculate the quantum orbits, namely by using the gradient of the classical BGK distribution. Instead of the characteristic system (36)-(37) we would have the characteristis system

$$\frac{dx}{d\tau} = \pm\frac{1}{\mathcal{N}_0}\frac{\partial f_0}{\partial p}$$
$$\frac{dp}{d\tau} = \mp\frac{1}{\mathcal{N}_0}\frac{\partial f_0}{\partial x},$$

with

$$\mathcal{N}_0 = \sqrt{\left(\frac{\partial f_0}{\partial p}\right)^2 + \left(\frac{\partial f_0}{\partial p}\right)^2}$$

the normalization factor. The critical points, since $f_0(x,p) = F_0(\mathcal{E})$, are given by

$$\frac{\partial f_0}{\partial p} = pF_0'(\mathcal{E}) = 0$$
$$\frac{\partial f_0}{\partial x} = E_0(x)F_0'(\mathcal{E}) = 0.$$

This system, in addition to the usual critical points at $p = 0$, is also solved by the critical lines along which $F_0'(\mathcal{E}) = 0$. However, since $F_0'(\mathcal{E})$ appears as a common factor in both equations, these critical lines do not affect the structure of the classical phase-space orbits (i.e., the contour lines of the distribution function) in their vicinity. In fact, they are phase-space orbits themselves. As the quantum characteristic system (39)-(40) is considered, the first-order perturbation terms break the critical lines into a discrete set of critical points, all lying near the critical lines. With the help of asymptotic analysis, these critical points could be obtained to first order in ε. The two critical points lying in the region of classically trapped particles (number 7 and 8), instead, are entirely due to the quantum effects and would be missed by the asymptotic analysis.

These considerations are confirmed as we looked at the behaviour of the critical points as $\varepsilon \to 0$. The critical points number 7 and 8 didn't move significantly, while the other critical points moved closer and closer to the critical lines. None of the critical points, however, disappears in the $\varepsilon \to 0$ limit. This is a subtle point, most probably related to the transition from the quantum to the classical behaviour, and to the validity of the semiclassical limit.

We would also like to note that the presence and the location of these additional critical points is directly related to our choice of the zero-order classical BGK equilibrium or, more precisely, to the boundary condition (30)-(31) that we have imposed on the distribution function at $x = 0$. If, as a boundary distribution, we had chosen a function with a monotone behaviour with respect to the energy (such as a Maxwellian), the equation $F_0'(\mathcal{E}) = 0$ would be satisfied only on the line $p = 0$, and the two sets of critical points that we have illustrated earlier would be absent. As we shall see, the additional critical points of Table I strongly affect the topology of the phase-space orbits in their vicinity.

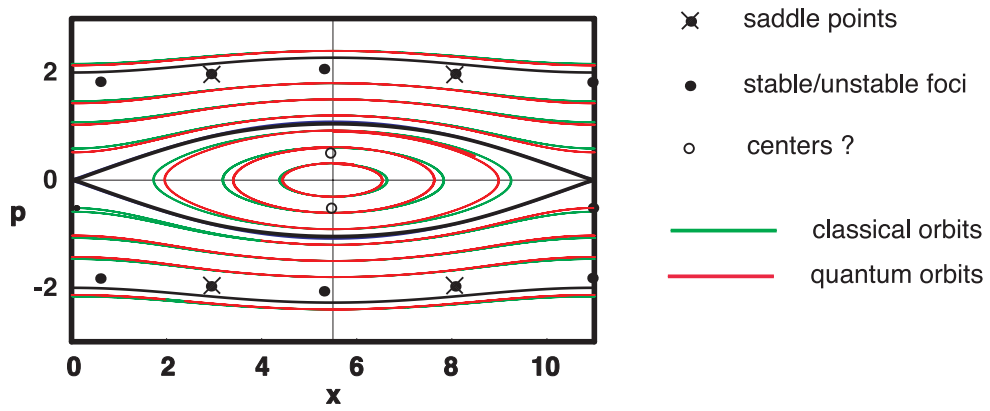

Figure 4: Classical and quantum phase-space orbits for $\varepsilon = 0.1$.

This shows how the structure of the quantum phase-space orbits is determined not only by the potential, as in classical systems, but also by the distribution which is introduced on it.

We now examine different families of quantum phase-space orbits and compare them with their classical counterparts. We first look at those orbits which never get close to the new critical points. These orbits, shown in Figure 4 for $\varepsilon = 0.1$, appear as "natural" quantum corrections to the classical ones. On the graph, the critical points reported in Table I are also shown. These phase-space orbits are clearly grouped into open and closed orbits, divided by two separatrices, very close to the classical separatrices. On the graph, each quantum orbit (red line) is shown together with the classical orbit (green line) that passes through the same point, at $x = L/2$. In general, the classical orbits tend to be broader, but the difference is very small.

Next, we examine the quantum orbits which pass close to the critical points at $p > 0$, near the critical lines. For this family of orbits, various situations are possible. The orbit in Figure 5(A) starts far from the critical point and behaves like the open orbits of Figure 4. In Figure 5(B), instead, two different orbits are shown: one spirals around the critical point number 5, the other spirals alternatively around the critical point number 1 and the critical point number 11, which are to be identified because of periodicity. The orbits of Figures 5(C) and 5(D) start just above the critical point number 5, but eventually enter the basin of attraction of the critical points number 1 and number 11, though with a different path.

Finally, in Figure 6, we show a quantum orbit which loops about critical point number 7, together with its classical counterpart. This orbit seems to behave like a truly closed orbit.

The phase-space orbits near the quantum critical points exhibit strong non-classical behaviour. This may be due to the nature of our perturbation approach, which destroys

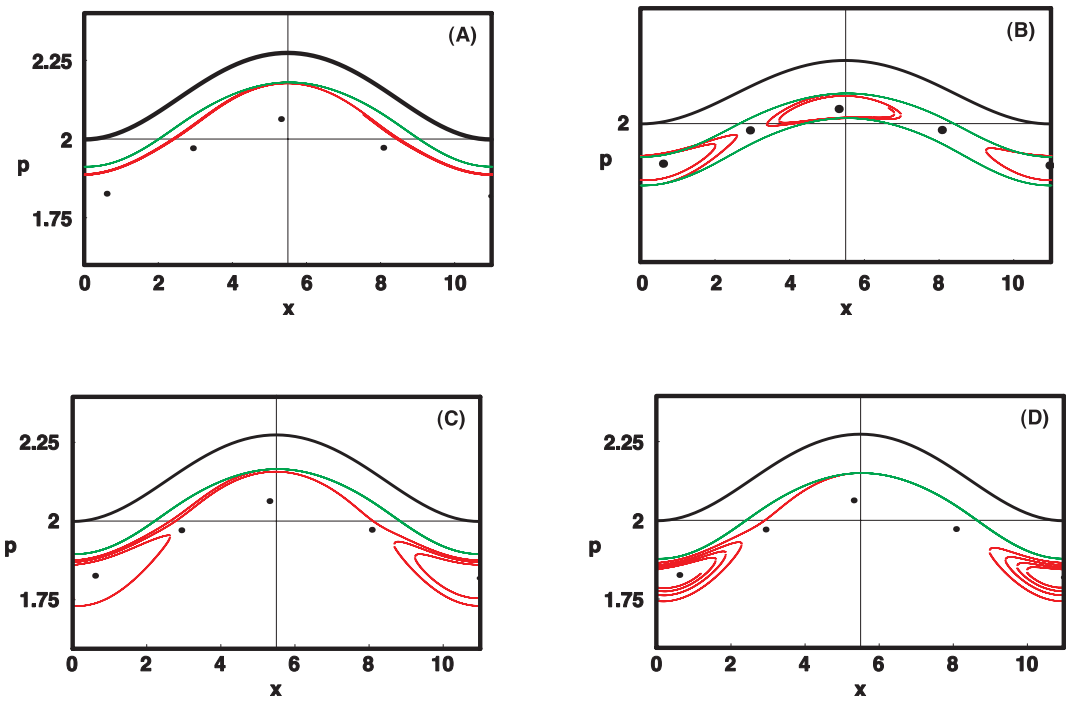

Figure 5: Classical (green lines) and quantum (red lines) phase-space orbits for critical points 1,3,5,9 and 11 for $\varepsilon = 0.1$.

the Hamiltonian structure of full quantum kinetic equations, or simply to the persistence of the quantum nature of the solutions at small values of ε. At this stage, we leave the question open, hoping that an answer will be found by analyzing the full quantum system.

5 Conclusions and Outlook

We have studied the steady-state solutions of the Wigner-Poisson system (QBGK equilibria) by a perturbative approach near a classical solution. We have obtained expressions for the first-order Wigner function and electrostatic potential which are almost analytical. We have also introduced a phase-space description through the isolines of the Wigner function. Some of the quantum phase-space orbits appear as natural corrections to the classical orbits while others exhibit strong non-classical behaviour also for very small values of ε.

As a next step, the study of the full quantum system will be performed, which requires the numerical solution of the nonlinear set of discretized equations. An investigation of the quantum effects on periodic travelling structures (BGK and QBGK modes, with non-zero phase velocity) should also be performed

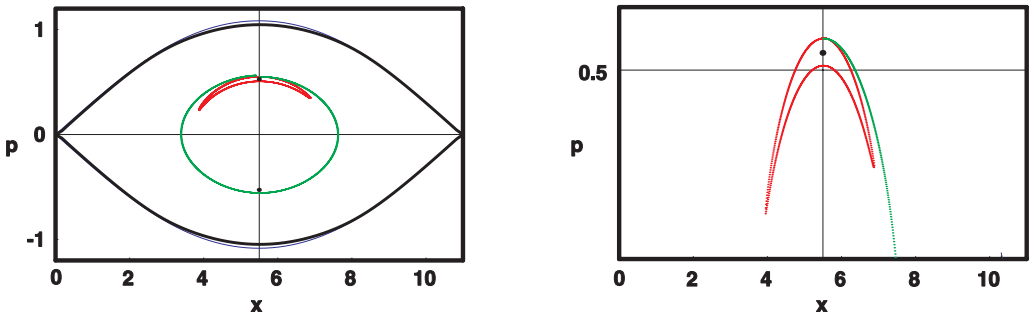

Figure 6: Classical (green line) and quantum (red line) phase-space orbits for critical point 7 for $\varepsilon = 0.1$. Figure 6B is a blow-up of Figure 6A.

References

[1] Vlasov, A. On the Kinetic Theory of an Assembly of Particles with Collective Interaction. J. of Phys. **1945**, *9*, 25-40.

[2] Bernstein, I. B.; Greene, J. M. ; Kruskal, M. D. Exact Nonlinear Plasma Oscillations. Phys. Rev. **1957**, *108*, 546-550.

[3] Buchanan, M. ; Dorning, J. J. Nonlinear Electrostatic Waves in Collisionless Plasmas. Phys. Rev. E **1995**, *52*, 3015-3033.

[4] Lange, H.; Toomire, B.; Zweifel, P.F. Quantum BGK modes for the Wigner-Poisson system. Transport Theory and Stat. Phys. **1996**, *25*, 713-722.

[5] Arnold, A. ; Markowich, P. The periodic quantum Liouville-Poisson problem, Bollettino U.M.I. **1990**, *7*, 449-484.

[6] Zweifel, P. F. The Wigner transform and the Wigner-Poisson system, Transport Theory and Stat. Phys. **1993**, *22*, 459.

[7] Neunzert, H. The "Nuclear" Vlasov equation. Methods and results that can(not) be taken over from the "Classical" case, Il Nuovo Cimento **1985**, *87A*, 151-161.

[8] Marinov, M. S.; Segev, B., Quantum Tunneling in the Wigner Representation. Phys. Rev. A **1996**, *54*, 4752-4762.

[9] Maitra, N. T.; Heller, E. J. Semiclassical Perturbation Approach to Quantum Reflection. Phys. Rev. A **1996**, *54*, 4763-4769.

[10] Manfredi, G. How to Model Quantum Plasmas? *quant-ph*/0505004

[11] Demeio, L. Perturbative approach to Quantum BGK Modes, Proc. VI Congresso SIMAI, Chia Laguna (CA-Italy) May 27-31, 2002.

[12] Demeio, L.; Holloway, J. P. Numerical Simulations of BGK Modes. Journal of Plasma Physics **1991**, *46*, 63-84.

[13] Demeio, L. A numerical study of linear and nonlinear superpositions of BGK modes, Transport Theory and Stat. Phys. **2001**, *30*, 457-470 .